Geophysical Research Letters

Supporting Information for

Different trends in Antarctic temperature and atmospheric CO_2 during the last glacial

Peisong Zheng[1, 2], Joel B. Pedro[3,4], Markus Jochum[5], Sune O. Rasmussen[6], Zhongping Lai[1, 7 *]

[1] Guangdong Provincial Key Laboratory of Marine Biotechnology, Institute of Marine Sciences, Shantou University, Shantou 515063, China.

[2] School of Earth Sciences, China University of Geosciences, Wuhan 430074, China.

[3] Australian Antarctic Division, Kingston, Tasmania, Australia.

[4] Australian Antarctic Program Partnership, University of Tasmania, Hobart, Tasmania, Australia.

[5] TeamOcean, Niels Bohr Institute, University of Copenhagen, Copenhagen, Denmark.

[6] Centre for Ice and Climate, Section for the Physics of Ice, Climate, and Earth, Niels Bohr Institute, University of Copenhagen, Copenhagen, Denmark.

[7] Three Gorges Research Center for Geohazards of MOE, China University of Geosciences, Wuhan 430074, China.

Contents of this file

Introduction

This document presents the supporting material for the temperature and CO_2 results. In Text S1 we discussed the sensitivity of the observed difference between CO_2 and Antarctic temperature to the influence of gas diffusion, ice diffusion, the choice of timescale, and the varying delta-age. The results support our conclusion in the main text.

Figure S1 to S4 and Table S1 are supporting information for temperature results, Figure S1 shows the 'temperature overshoot', Figure S2 to S4, and Table S1 show the exponential fit for the AIMs and the analysis results for individual ice cores of the five-core averaged data. Figure S5 to S12 show the searched maximums/minimums for different CO_2 records, the significant test for the nHS CO_2 amplitude, and the results of CO_2 sensitivity test.

Text S1. Sensitivity test for CO_2 results

Three main factors can unevenly smooth the CO_2 record and influence the CO_2 amplitude and rate, the first is the varying resolution, with lower resolution reducing the CO_2 amplitude. The second is the different firn diffusion and enclosure characteristics between ice core sites (Bereiter et al., 2012). The third is the diffusion in ice (Ahn et al., 2008), which unevenly smooth CO_2 in different depths, with deeper ice being smoothed more (Ahn et al., 2008).

For the influence of varying resolution, the 300 yr window we applied for moving averages is larger than the 88% quantile of the resolution of MIS-3 section of composite CO_2 data, thus it is capable to reduce the effect of varying resolution by removing the

high-frequency signal. Our conclusion also holds when the smoothing length increased to 500 yr (Figure S12), suggest the varying record resolution has negligible influence on our finding.

To evaluate the influence of different enclosure characteristics between ice cores, we performed a one to one comparison for the trend of Talos CO_2 data (in AICC2012 timescale; Bereiter et al., 2012, 2015) and Talos $\delta^{18}O$ data (in AICC2012 timescale; Figure S8; Landais et al., 2015; Stenni et al., 2011; Veres et al., 2013), both records are smoothed by 300 yr moving average before searching maximums/minimums. Due to the uneven spacing between Greenland climate transition (in GICC05 timescale; Rasmussen et al., 2014) and the AIM peaks/valleys of the Talos $\delta^{18}O$, we manually determined the $\delta^{18}O$ maximums and minimums. The CO_2 maximums/minimums are directly searched in the smoothed data by the same method as the main text. The two-side significance of the BPS warming rate slope is 85.09%, probably due to reduced event numbers. But it is still significantly higher than the two-side significance of CO_2 slope, which is only 54.44% (Figure S8), The result thus supports the conclusion that the CO_2 trend is less sensitive to varying background climate than the temperature trend and indicates the site-dependent gas diffusion does not change our conclusion.

The result also shows the varying of delta-age between gas and ice does not change our conclusion. As the BPS warming rate in Talos $\delta^{18}O$ is calculated in GICC05 timescale (Svensson et al., 2008), and the CO_2 timescale is synchronized to it by CH_4 synchronization (Veres et al., 2013). Thus, the influence of delta-age is largely reduced in this experiment.

To evaluate the influence of depth/time-dependent ice diffusion, we compared the MIS-3 CO_2 amplitudes with the one from the newly recovered high-resolution (ca. 200 yr) EDC CO_2 data of MIS-10, 11, and 12 (in AICC2012 timescale, Figure S9, S10; Nehrbass-Ahles et al., 2020). The EDC CO_2 amplitudes are in line with Talos (Figure S10), suggesting that the CO_2 amplitude is not significantly reduced due to ice diffusion. Moreover, we compared the trend between new EDC CO_2 with the EDC δD (in AICC2012 timescale, Figure S9, the CO_2/δD maximums and minimums are manually determined from the 300 yr smoothed data), the two-side significance of CO_2 and temperature rate slope is 58.55% and 89.20% respectively, support our conclusion and indicate the influence of ice diffusion is negligible. The result also suggests the different CO_2 and Antarctic temperature trend exist beyond the last ice age.

The above experiments also suggest the different CO_2 and Antarctic temperature sensitivity to varying background climate is not biased by the use of timescale, as our results show high consistency between different combinations of records: composite CO_2 data (AICC2012) vs five core averaged $\delta^{18}O$ (WD2014), Talos CO_2 (AICC2012) vs Talos $\delta^{18}O$ (GICC05); EDC CO_2 data (AICC2012) vs EDC δD data (AICC2012).

To further test the robustness of our conclusion we also used alternative Methods to compare the slopes of CO_2 and temperature rates: in each iteration, for each CO_2/temperature rate, we draw values from their normal distribution defined by their value with standard deviation set as their 1-sigma uncertainty. Then we normalized the randomly generated CO_2/temperature rates to zero mean and unit variance separately and linear fit the AIM age against the rates and record the fitted slope. After 100,000

iterations, we compare the distribution of the slope of CO_2 and temperature rates. For all three combinations: five-core average $\delta^{18}O$ vs composite CO_2 data, Talos CO_2 vs Talos $\delta^{18}O$, and new EDC CO_2 data vs EDC δD, the median temperature rate slope is larger than the CO_2 rate slope (Figure 3e, 3f, S11). This result is supported by a t-test that shows the CO_2 and temperature rate slope are significantly different (at 95% significance level) in all three cases.

We also explored whether our results are sensitive to the change in smoothing Methods, or the use of detrended data (composite CO_2 data is used, with all 10 events). When the detrended CO_2 data is used (created by removing the long-term signal, represented by the 20,000 yr moving average smoothing, from the composite CO_2 record), the two-side significance for the slope of CO_2 rate is 85.99% (Figure S12). We create a spline-fitted CO_2 record by fitting the composite CO_2 record by smooth spline with cut-off period of 500 yr (Bereiter et al., 2012). The two-side significance of the slope of CO_2 rates is 89.62% (Figure S12). In both cases, the two-side significance of the CO_2 rate slope is similar to what we reported in the main text, and the significant difference between HS and nHS CO_2 rate is not detected (by t-test, at 95% significance level), a significant difference between HS and nHS CO_2 overshoots are confirmed (by t-test, at 95% significance level).

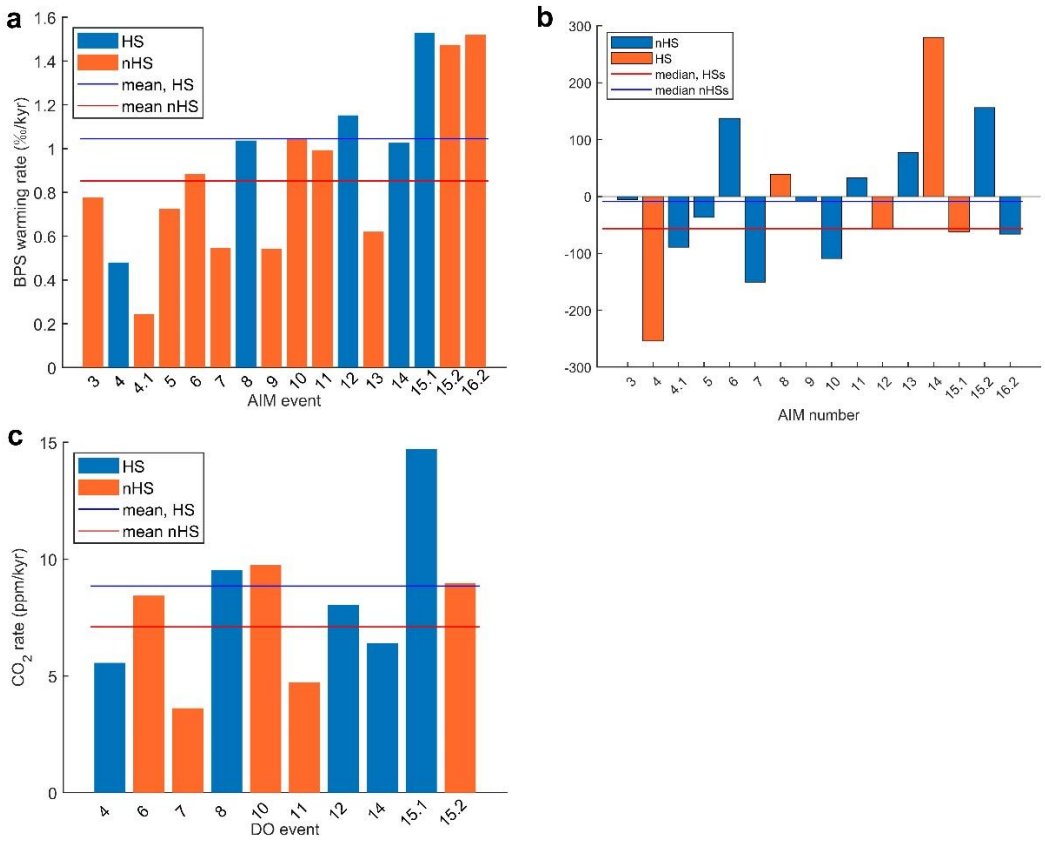

Figure S1. The bar chart for the rate and time of temperature and CO_2 rise. **a.** The BPS warming rates. **b**. the Antarctic warming overshoot. **c.** CO_2 rates.

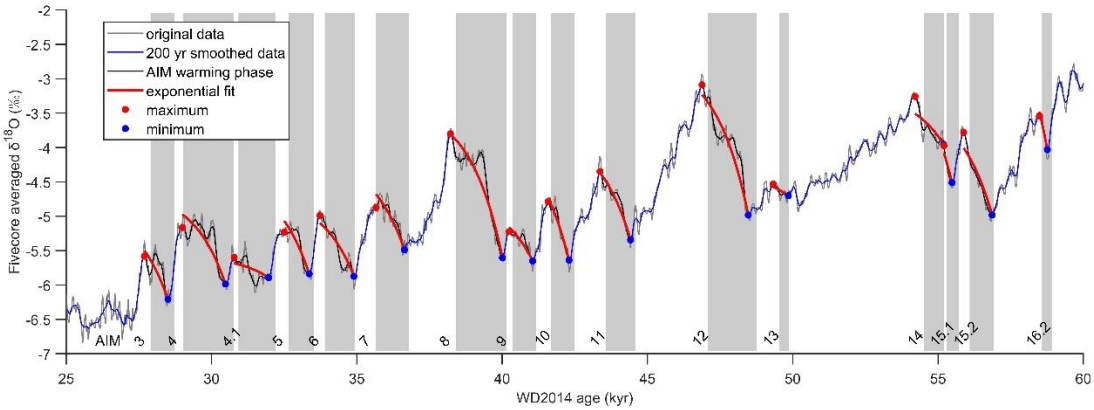

Figure S2. The exponential fit for the AIMs on the five-core averaged data (Buizert et al., 2018). Gray vertical bars mark the Greenland stadials.

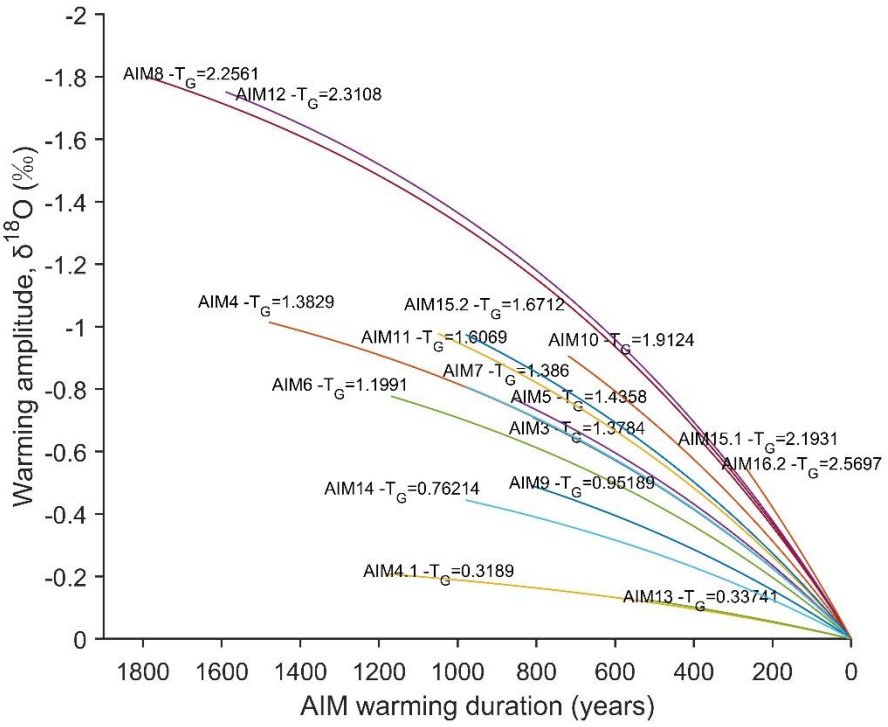

Figure S3. Comparison of the $-T_G$ of the AIMs. The $-T_G$ is calculated from the five-core averaged data (Buizert et al., 2018).

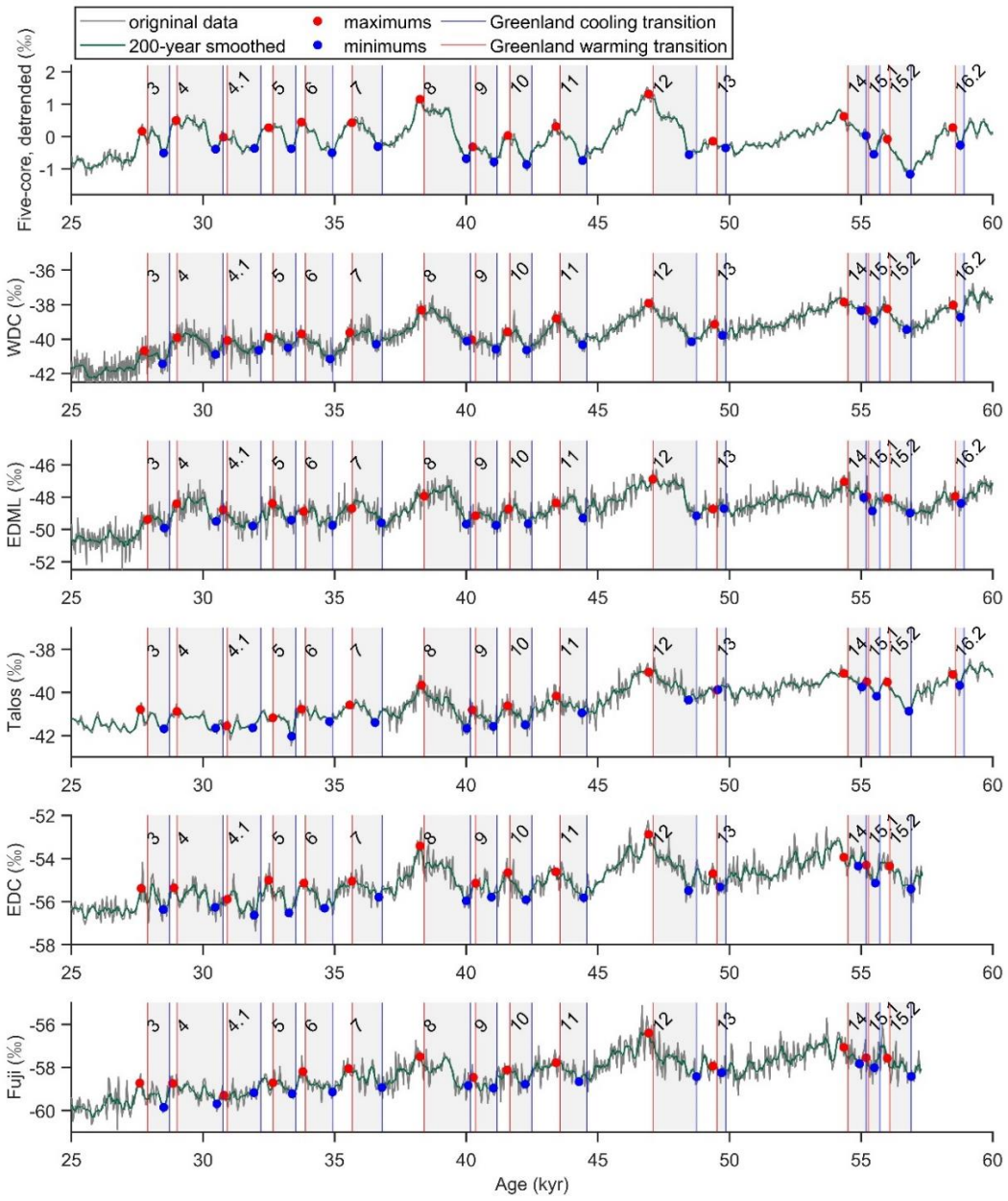

Figure S4. Example for the searched maximums and minimums. From top to bottom: the detrended five-core averaged data (Buizert et al., 2018), West Antarctic Ice Sheet Divide (WDC; WAIS, 2013, 2015), European Project for Ice Coring in Antarctica (EPICA) in the interior of Dronning Maud Land (EDML; EPICA, 2006), Talos Dome (Landais et al., 2015; Stenni et al., 2011), EPICA Dome C (EDC; EPICA 2004), and Dome Fuji (Fuji; Kawamura et

al., 2007; Watanabe et al., 2003). All these ice cores are on WD2014 time scale(Buizert et al., 2018).

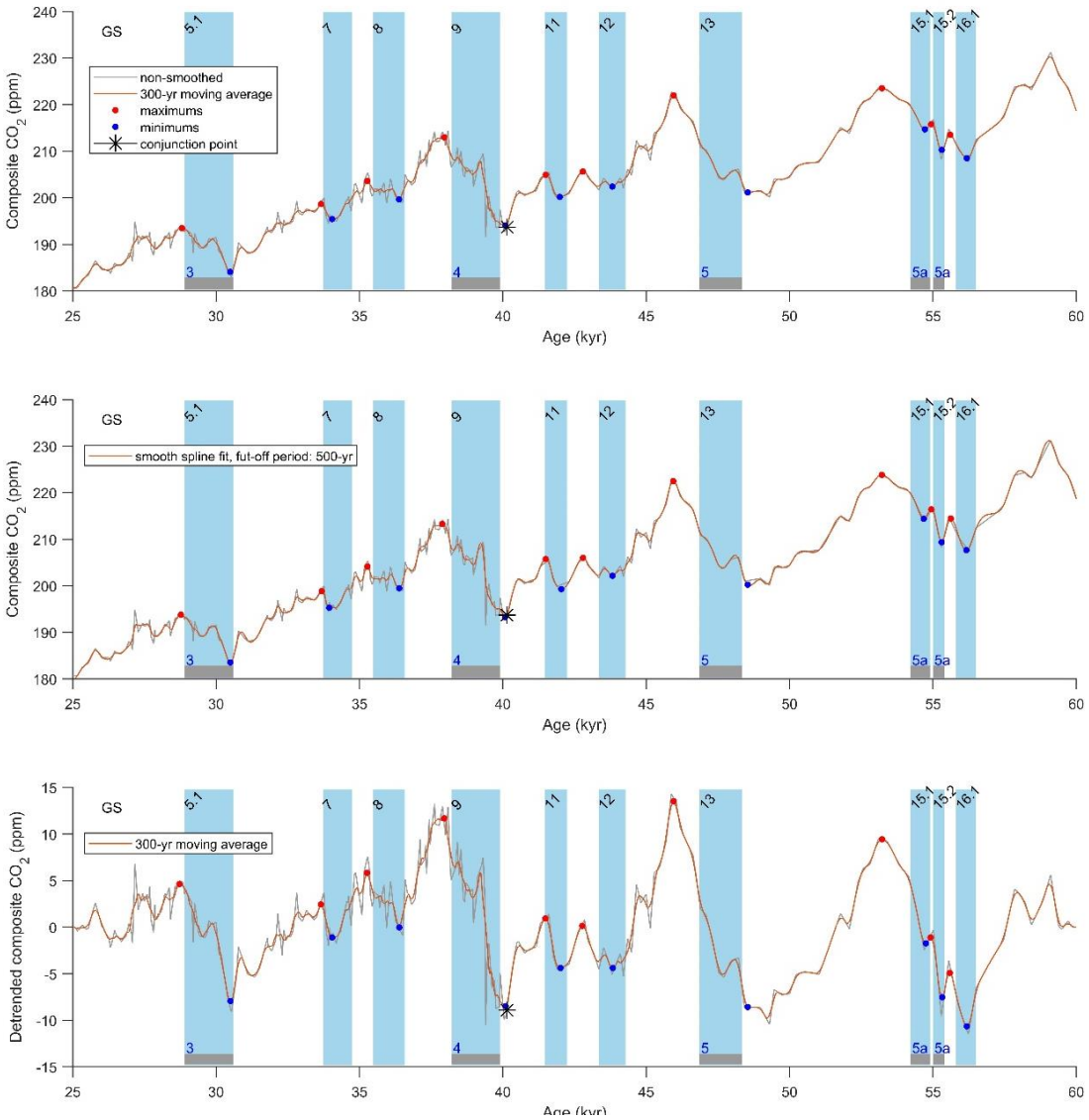

Figure S5. Example of the maximums and minimums searched in the CO_2 records. From top to bottom: the composite CO_2 (Bereiter et al., 2012), smooth spline fitted composite CO_2 data, and the detrend composite CO_2 data. The time of Greenland stadial and Heinrich events are marked by blue and gray bars respectively.

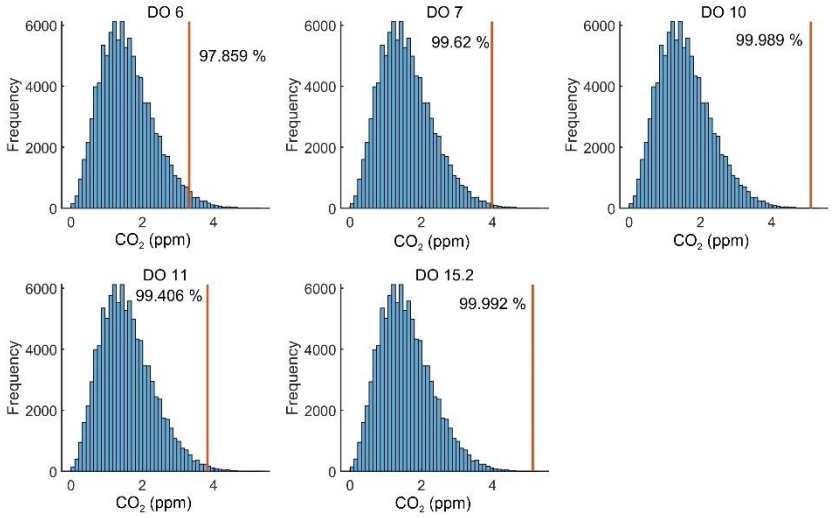

Figure S6. The significance of the CO_2 amplitude for the nHSs. For all five events, the amplitude of CO_2 rise is significantly larger than the uncertainty of amplitude (in 95% level). Here the distribution of the uncertainty of amplitude is calculated by adding the uncertainty of two arbitrarily selected CO_2 data points in the composite CO_2 record and repeat the operation100,000 times.

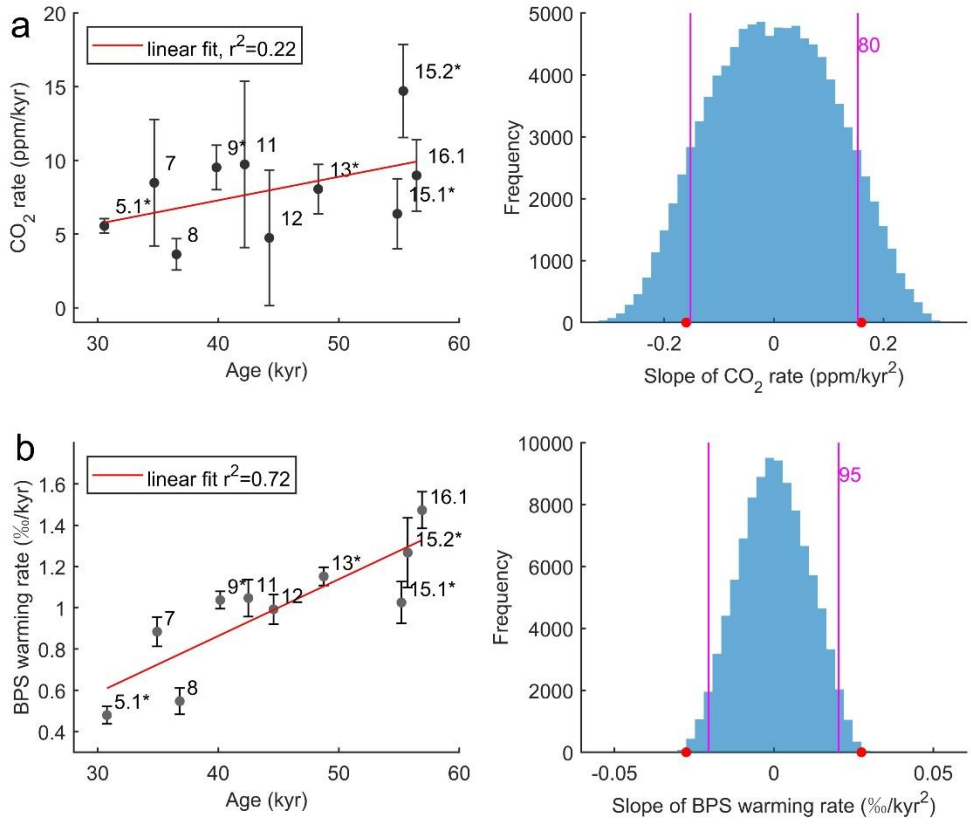

Figure S7. Comparison of CO_2 and temperature trend of composite CO_2 data (Bereiter et al., 2015) and Antarctic five-core average $\delta^{18}O$ (Buizert et al., 2018) for the same GSs. **a.** The CO_2 rate plot against the age of corresponding GS (left); the two-side significance of the CO_2 rate slope calculated from randomly permuting the CO_2 rate 100,000 times (right). The error bar in the left shows the 95% CI of the CO_2 rate from the MC simulation. **b.** Same as **a** but for five-core average $\delta^{18}O$ data. The two-side significance of the CO_2 and warming rate slope are 82.43% and 99.87% respectively.

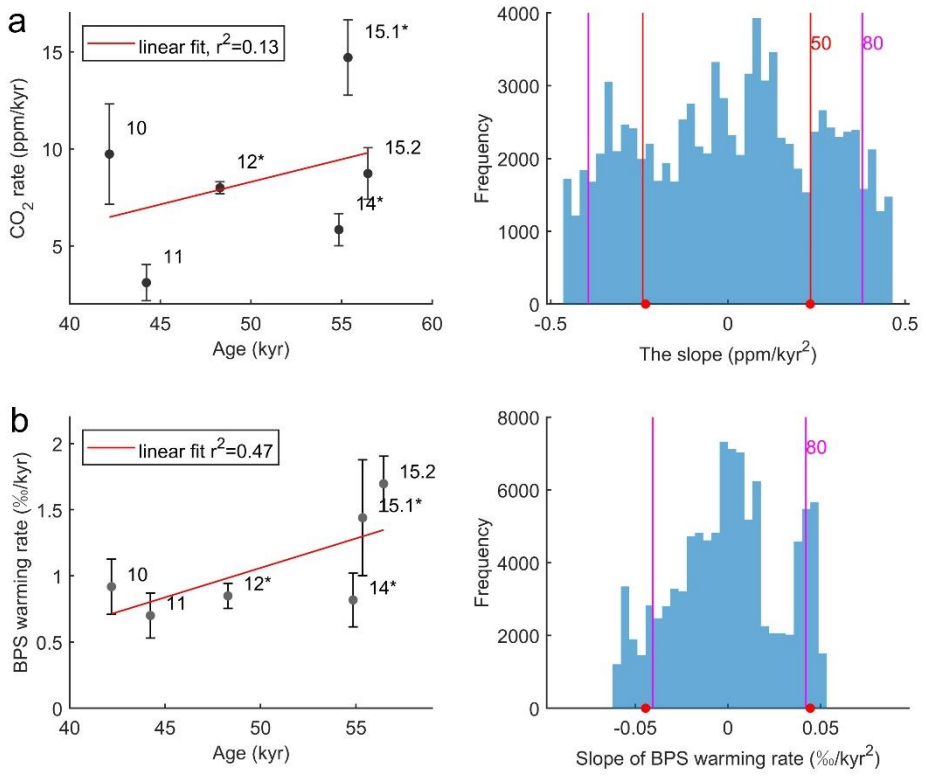

Figure S8. Comparison of Talos Dome CO_2 and temperature trend. **a.** The CO_2 rate plot against the age of corresponding GS (left); the two-side significance of the CO_2 rate slope (right). The uncertainty of the CO_2 rate in the left is derived from the uncertainty of the amplitude, which is the sum of the corresponding uncertainty of maximums and minimums (interpolated from the uncertainty of CO_2 data at the time of maximums/minimums; Bereiter et al., 2015; Bereiter et al., 2012). **b.** Same as **a** but for Talos $\delta^{18}O$ data (Landais et al., 2015; Stenni et al., 2011). The uncertainty of the warming rate is derived from the uncertainty of the amplitude, and the uncertainty of $\delta^{18}O$ maximums and minimums are set as the standard deviation of the residual, which is the isotope difference between the unsmoothed and 300 yr smoothed data.

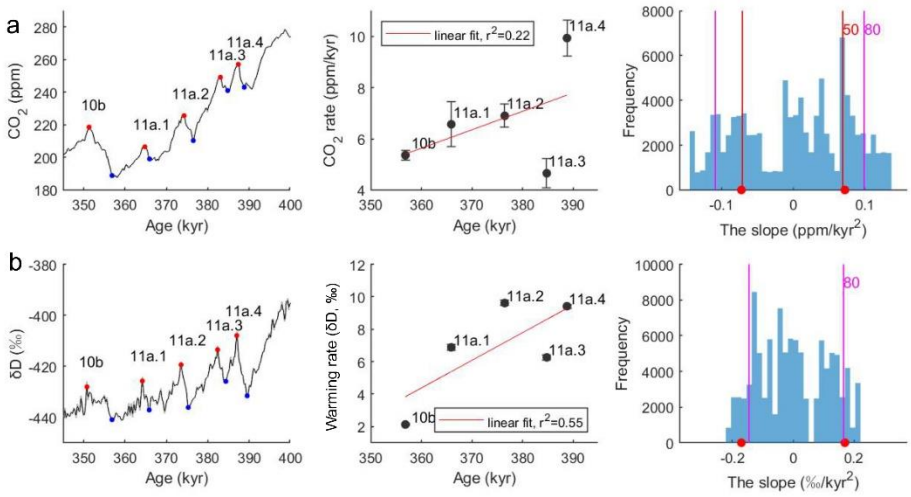

Figure S9. Comparison of EPICA Dome C CO_2 and temperature trend during 350 to 400 kyr BP. **a.** The CO_2 maximums and minimums manually picked in the 300 yr moving average smoothed new EDC CO_2 data (Nehrbass-Ahles et al., 2020) (left), the uncertainty of the maximums/minimums are interpolated from the uncertainty of CO_2 data (Nehrbass-Ahles et al., 2020) at the time of maximums/minimums; The CO_2 rate plotted against the age of CO_2 rise (defined as the age of corresponding CO_2 minimum, middle), the uncertainty of the CO_2 rate is derived from the uncertainty of the amplitude; the two-side significance of the CO_2 rate slope (right). **b.** Same as **a** but for EDC δD data (EPICA, 2004). The uncertainty of the maximums and minimums are set as the standard deviation of the residual, the residual is the δD difference between the unsmoothed and 300 yr smoothed data. We identified the CO_2 and temperature rise with the corresponding carbon dioxide maximum labeled by previous research (Nehrbass-Ahles et al., 2020). The CO_2 and δD record are both in AICC2012 timescale.

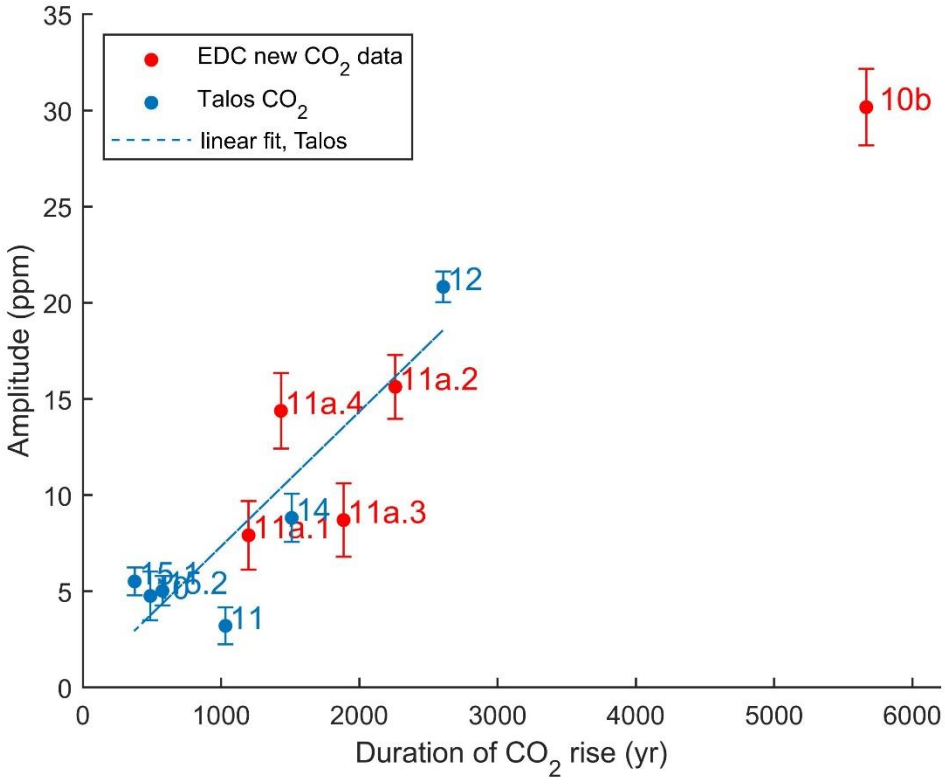

Figure S10. Comparison of the amplitude of CO_2 rise of Talos CO_2 data (Bereiter et al., 2012) and the new EDC CO_2 data (Nehrbass-Ahles et al., 2020). The CO_2 rises in new EDC data are labeled in their corresponding CO_2 maximum following previous research (Nehrbass-Ahles et al., 2020).

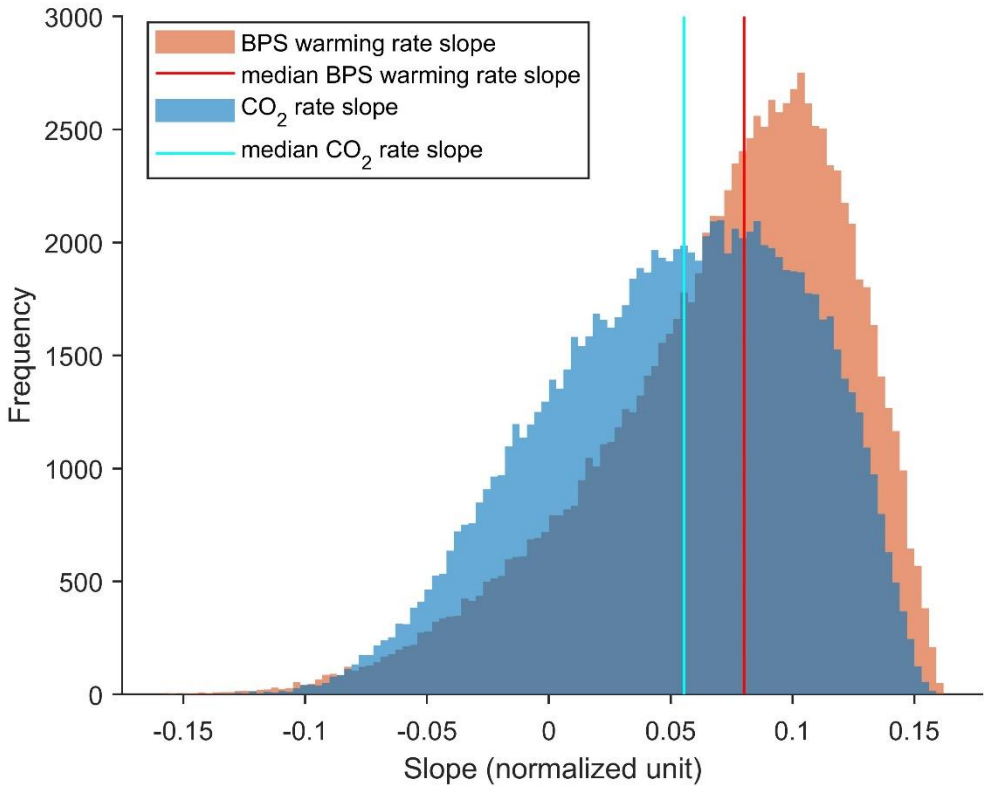

Figure S11. The distribution of randomly generated CO_2 and temperature rate slope for the Talos data. The CO_2 data is from (Bereiter et al., 2012), the $\delta^{18}O$ data is from (Landais et al., 2015; Stenni et al., 2011). The randomly generated rates have been normalized to zero mean and unit variance before linear fit to calculate the slope.

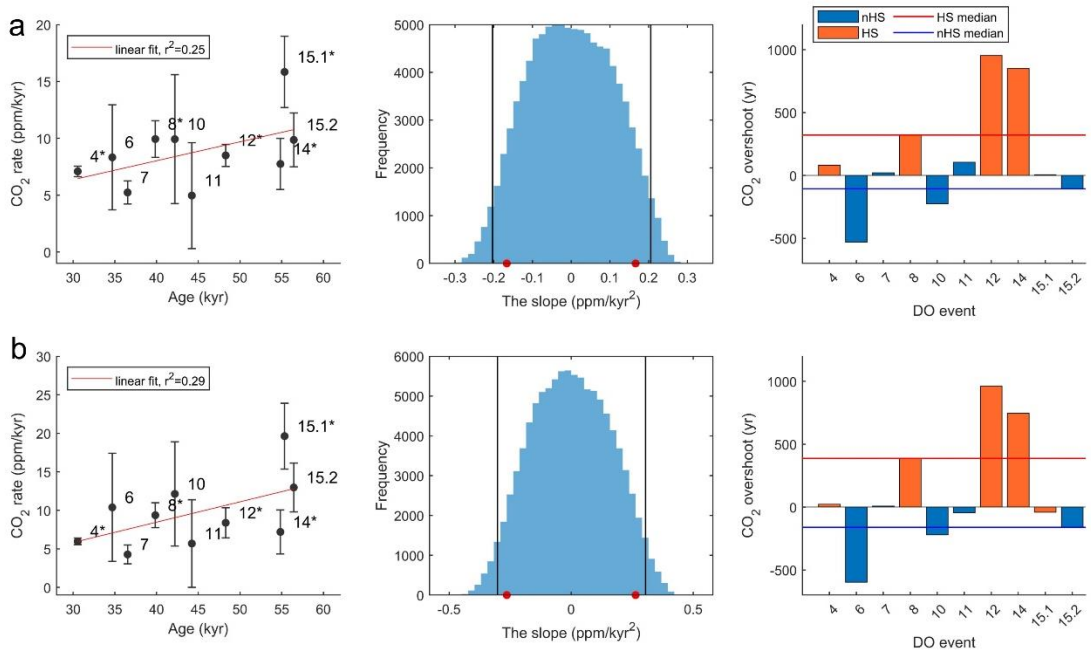

Figure S12. CO_2 results from the detrended and smooth spline fitted composite CO_2 data (Bereiter et al., 2015). **a.** results for detrend data: CO_2 rate plotted against the age of the corresponding AIM (left), error bar show the 95% CI; two-side significance for the slope of the CO_2 rates, the vertical black lines mark the 95% confidence level (middle); The CO_2 overshoot (right). **b.** same as **a** but for the smooth spline fitted data, with cut-off period of 500 yr (Bereiter et al., 2012).

Record	1 sigma uncertainty of MC simulation (‰)	Significance of two-side, BPS warming rate slope (%)	t-test, HS vs nHS BPS warming rate (1 for significant 0 for not significant)	Significance of two-side, warming rate slope (%), Antarctic perspective	t-test, HS vs nHS warming rate (1 or 0), Antarctic perspective	two side significance of the -T_G slope (%)
Five-core Antarctic perspective	0.12	–	–	99.65	0	–
Five-core detrended	0.12	99.98	0	99.40	0	94.59
WDC $\delta^{18}O$	0.36	99.94	0	99.91	0	–
EDML $\delta^{18}O$	0.43	99.92	0	98.37	0	–
Talos $\delta^{18}O$	0.30	99.92	0	99.49	0	–
EDC $\delta^{18}O$	0.33	98.73	0	96.37	0	–
Fuji $\delta^{18}O$	0.33	97.62	0	99.89	0	–

Table S1. The analysis results for the AIM warming from Antarctic perspective, the detrended five-core averaged data, and the individual ice cores that go into the five-core averaged data (Buizert et al., 2018). Note that the two-side significance for the -T_G slope for the detrended data is slightly below the threshold we set, but as the value is very high, we still suggest a significantly lowered -T_G throughout the MIS-3. The exponential fit and -T_G calculation for the individual ice cores of the five-core averaged record is impeded by the high noise level.